Research | Egyptian Journal of Agricultural Research | Plant Pathology

Antifungal activity of MgO and ZnO nanoparticles against powdery mildew of pepper under greenhouse conditions

Ahmed Mahmoud Ismail[1] *and Mona Ebrahim Abd El-Gawad*[2]

Address
[1]*Plant Pathology Research Institute, Agricultural Research Centre, Giza, Egypt*
[2]*Cytogenetics Lab, National Gene Bank, Agricultural Research Centre, Giza, Egypt*
*Corresponding author: ***Ahmed. M. Ismail***, * ma.ah.ismail@gmail.com
Received: 01-10-2021; **Accepted**: 09-11-2021; **Published:** 29-11-2021 doi, 10.21608/ejar.2021.96252.1150

ABSTRACT
Powdery mildew disease of peppers (*Capsicum annuum* L.) caused by *Oidiopsis sicula* is the most damaging disease in the field and greenhouse. Chemical control has been widely used for the control of powdery mildew. To minimize the deleterious impacts of fungicides, the present study aimed to evaluate the antifungal effect of different concentrations (100, 150 and 200 mg/L) of MgONPs and ZnONPs against powdery mildew in comparison with the conventional fungicide penconazole (0.25 ml/L) under greenhouse conditions. The synthesis and characterization of MgO and ZnONPs were carried out. Dynamic light scattering (DLS) analysis revealed the presence of MgONPs and ZnONPs at the nanoscale level with a size average of 52.97 nm ± 1.43 S.D and 79.45 nm ± 1.74 S.D, respectively. Two foliar sprays were applied at two-week intervals on pepper plants cv. Dolma, naturally infected with powdery mildew in the three greenhouses of El -Dokki (GH-1), Toukh (GH-2) and El-Haram (GH-3). Both MgONPs and ZnONPs markedly reduced disease severity (DS) and area under the disease progress curve (AUDPC) at a concentration of 200 mg/L. Statistical analysis showed a significant ($p<0.05$) difference between treatments in the three greenhouses as well as between means of combined treatments. Scanning electron micrographs confirmed that MgONPs and ZnONPs caused inhibition and alterations in the treated fungal structures. Pepper plants treated with penconazole displayed the highest peroxidase activity and recorded 1.229 ΔA422/10 sec/g FW. While, the highest polypheneloxidase activitiy was obtained by MgONPs with value reached 0.283 ΔA495/10 sec/g FW . Out of all treatments, MgONPs were the superior in increasing total chlorophyll at the three applied concentrations, with values of 74.81, 82.94, and 91.19 mg/g FW, respectively. Cytotoxic investigations exhibited the clastogenic nature of MgONPs, ZnONPs, and penconazole. The obtained results are encouraging and emphasize the recognition of MgONPs and ZnONPs as a viable alternatives to conventional strategies.
Keywords: Cytotoxic, MgONPs, ZnONPs, pepper, powdery mildew

INTRODUCTION
Powdery mildew disease of pepper is the most damaging diseases in the field and greenhouse caused by *Oidiopsis sicula* Scalia (Syn. *Oidiopsis taurica* E. S. Salmon; telemorph *Leveillula taurica* (Lev.) G. Arnaud). However, cleistothecia of the telemorph *L. taurica* have been found on other host plants, but have not been reported on peppers (Pernezny *et al.,* 2003). In terms of pepper production, the disease is becoming a major issue, since it causes large losses in producing regions (Guigón-López *et al.,* 2020). Powdery mildew has been treated with chemical control due to its efficiency. The use of fungicides on a regular basis exposes the environment to chemicals, which can have harmful effects on ecosystems and wildlife (Wightwick *et al.,* 2010). Different genera of bacteria and fungi as biocontrol agents have also been used for controlling the disease (Guigón-López *et al.,* 2018; Abdel-Kader *et al.,* 2012). However, biocontrol agents are not highly effective and require to be combined with other alternatives in integrated management strategies for strong and stable control of pepper powdery mildew (Guigón-López *et al.,* 2020). Therefore, nanomaterials as new alternatives are sought in the area of nanobiotechnology applications.

The nanoparticles (NPs) represent a new approach for the development of alternatives to fungicides due to their unique physical and chemical properties, which often differ significantly from their bulk form (Köhler *et al.,* 2008). Nanoparticles of metal oxides such as MgO and ZnO, which have recently attracted significant interest due to their strong antimicrobial characteristics and minimal toxicity towards mammalian cells, are now being utilised to treat bacterial and fungal plant pathogens that cause some diseases in plants (Alghuthaymi *et al.,* 2021; Kalia *et al.,* 2020; Elmer and White, 2018; Gunalana *et al.,* 2012). According to the U.S. Food and Drug Administration, magnesium oxide nanoparticles (MgO) and Zinc oxide (ZnO) were recognized as safe substances and can be used as disinfection agents and promising in medical therapeutics at nanoscale (FDA 2016; Krishnamoorthy et al., 2012). In agriculture, MgONPs have also the potential as antibacterial agents against *Ralestonia solanacearum* (Cai *et al.,* 2018b; Imada *et al.,* 2016), soil-borne fungal pathogens (Chen *et al.,* 2020; Parizi *et al.,* 2014), and foodborne pathogens (Jin and He, 2011). The antifungal potency of ZnONPs has been well recognized against phytopathogenic fungi such as *Peronospora tabacina* (Wagner *et al.,* 2016), *Alternaria alternata* and *Colletotrichum gloeosporioides* (Malandrakis *et al.,* 2019). The antifungal potency of MgONPs and ZnONPs against powdery mildew diseases is still in its infancy with very little literature and proven mechanistic details. As a result, the current study was carried out during the season of 2020-2021 to synthesise, characterise, and investigate the significant potential of MgONPs and ZnONPs

as alternative disease management strategies against powdery mildew in comparison to a conventional fungicide, as well as to determine their cytotoxic effect on treated pepper plants.

MATERIALS AND METHODS

Preparation and Characterization of MgONPs and ZnONPs:

To produce ZnO and MgO NPs, magnesium and zinc nitrate hexahydrates were employed as precursors. The coprecipitation technique employed sodium hydroxide (NaOH) as a precipitating agent. ZnO and MgO were co-precipitated using the technique of Tamilselvi *et al.* (2013). A PerkinElmer Lambada 950 UV/Vis spectrometer was employed for UV-vis spectroscopy of the produced MgO and ZnO NPs, with wavelength ranges between 300 and 600 nm. High-resolution transmission electron microscopy (HR-TEM) on carbon-coated copper grids using a JEOL instrument 1200 EX equipment operated at an appropriate accelerating voltage was used to investigate the morphology of MgO and ZnO NPs (kV). The Gatan Digital Micrograph was used to measure the lattice fringes in the fast-Fourier transform of HRTEM pictures. A Malvern Zetasizer Nano ZS 90 system was used to measure the size distribution and zeta potential (Malvern Inc., UK).

Greenhouse Experiments:

Three trials were carried out under greenhouse conditions during the seasons of 2020-2021 to evaluate the antifungal effects of MgONPs and ZnONPs in comparison with penconazole against powdery mildew of pepper caused by *O. sicula*. The locations of the greenhouses were in Giza; Eldokki (GH-1) and Elharam (GH-3), and (Kaliobyia), Toukh (GH-2). The trials were carried out on two-month-old pepper cv. Dolma, naturally infected with *O. sicula*. Plants were sprayed with MgONPs and ZnONPs at three concentrations of 100, 150, and 200 mg/L. The conventional fungicide (Topas100 EC; Syngenta), active ingredient penconazole, was included for comparison and used at the recommended rate (0.250ml/L). Each greenhouse received the same treatments mentioned above. Plants were sprayed two times at 2-week intervals. Control plants were sprayed with only tap water. All the recommended agricultural practises were applied in each greenhouse. Trials were carried out using randomized complete block design with three replicates. Ten plants were used for each replicate. Plants were grown on both sides of a soil ridge 0.5 m wide, and the distance between plants was 30 cm.

Disease Severity Assessment:

Disease severity was determined before spray (zero time) and 4 times with 7-days intervals. Severity was estimated by visual estimation of sporulating mildew colonies on fully expanded leaves from the middle part of each plant. Disease Severity (DS) % was visually recorded using the scale (0 to 6) as described by Spencer, (1977); whereas: 0 = No visible infection; 1 = 1 % or less; 2 = 2-5 %; 3 = 6-20 %, 4 = 21-40 % 5= > 40 %, and 6 = 100 % infected area of leaf. DS was calculated according to the equation described by Descalzo *et al.* (1990) as follow:

$$R = [\sum (a \times b)/N \times K] \times 100.$$

Where: R =disease severity %, a =number of infected leaves rated, b = numerical value of each grade, N =total number of examined plants, K = the highest degree of infection in the scale.

Area Under Disease Progress Curve (AUDPC) was calculated to compare amounts of disease among different treatments using the following equation of Pandey *et al.* (1989);

AUDPC = D [1/2(Y1 + Yk) + Y2 +Y3 +…+ Y (k-1)]

Where: D = days between readings, Y1 = first disease record, and YK = last disease record.

The Activity of Defence-Related Enzymes:

After 72 hours, the leaves of treated pepper plants were harvested and examined for peroxidase and polyphenoloxidase activity. The activity of polyphenoloxidase was determined using the method published by Matta and Dimond (1963). The peroxidase test (based on pyrogallol oxidation to purpyrogallin in the presence of H2O2) was performed using the method reported by Allam and Hollis (1972).

Estimation of Chlorophyll:

The amount of cholorphyll in each sample was measured at the end of the research. Cutting fresh leaves into little pieces, the pigments were removed by grinding the tissues in 80 percent acetone, then filtering to eliminate any debris, according to Porra (2005). Ten millilitres of acetone have been refilled. The optical density at 663 and 645 nm was measured using a Unico-2000 UV spectrophotometer to estimate the total chloroplast pigments (Unico Scientific, Hong Kong, China). Arnon's formula was used for determining chlorophyll concentration (Arnon, 1949).

Scanning Electron Microscopy (SEM):

SEM was used to observe the morphological changes of hyphae and spores of *O. sicula* in response to foliar spray with MgONPs and ZnONPs. Treated pepper leaves were collected 48 h after the first treatment. Samples were cut into sections (5 mm) and fixed to stubs using double-sided sticky tape, and sputter coated with gold-palladium. SEM micrographs were done using JEOL GM 5200 SEM microscope at Applied Center for Entomonematodes (ACE), Faculty of Agriculture, Cairo University, Giza, Egypt.

Cytological studies:

The seeds of treated and control pepper plants were germinated on moistened filter paper in Petri-dishes at room temperature. Root-tips (1-2 cm long) were collected and pretreated by fixing them in ethanol-glacial acetic acid (3:1). After 24 h, root tips were transferred to 70% ethyl alcohol and stored. The aceto-orcein staining method was used to stain the root tip cells as described by Sayed-Ahmed (1985). The fixed root-tips were washed thoroughly with distilled water, then squashed on dry clean slides and stained with a small drop of aceto-orcein stain. Scoring of the cytological criteria was carried out from at least five prepared slides, 400 cells of each. The prepared slides were used to determine the mitotic index and chromosomal aberrations (CA). The CA were visualized using vertical fluorescence microscope (Leica DM4 B) (Leica Microsystems, Germany) equipped with a cooled digital color camera (Leica DFC450C).

The mitotic index represented the percentage of divided cells to the total cells examined. Each mitotic phase's percentage is determined by dividing the number of cells in that phase by the total number of dividing cells. In dividing cells, the total number of CA was calculated. Cells having micronuclei (compact and non-compact), fragments, sticky binucleate cells, and laggards were among the abnormalities (Jacobs,1997).

Data Analysis:

The data of DS, AUDPC, MI and CA were subjected to analysis of variance (ANOVA) and treatment means were separated by Fisher's protected least significant difference (LSD). Data were analysed using statistics software SPSS 8·0 (SPSS).

RESULTS

Physicochemical Characterization of MgONPs and ZnONPs:

The HR-TEM representative image exhibited slight irregularly faceted particles with a predominantly cubic shape of MgONPs (Fig. 1A). The MgONPs showed aggregates connected in chains with a grape-like shape. The corresponding selected area electron diffraction (SAED) pattern showed visible lattice fringes correspond to the MgO in its surface through a high magnification view of single-particle (Fig. 1B, C). The synthesis of MgONPs was confirmed by UV visible spectroscopy technique in which the absorption spectra exhibited a peak at 325 nm for MgONPs (Fig. 1D). The results of DLS analysis revealed the presence of MgONPs at nanoscale level with a size average of 52.97 nm ± 1.43 S.D (Fig. 1E). The surface charge of the MgONPs showed a value of + 4.55 mv (Fig. 1F). The HR-TEM image reported in Fig (2A) showed that the synthesized ZnONPs appeared to be monodispersed as well as in aggregated form. The prevalent morphology was rod-shaped and occasional non-homogenous shape (Fig. 2A). SAED image obtained for ZnONPs has clear diffraction rings of ZnO (Fig. 2B), and distinct lattice fringes observed in HRTEM images of rod-like particles (Fig. 2C). The spectral analysis results indicated that maximum peak absorption was found at 355 nm confirming the synthesis of ZnONPs (Fig. 2D). The results of DSL revealed that ZnONPs were heterogeneously distributed with an average size of 79.45 nm ± 1.74 S.D (Fig. 2E) and recorded zeta potential of + 6.12 mv (Fig. 2F), indicating dispersion and moderate stability of ZnONPs in solution.

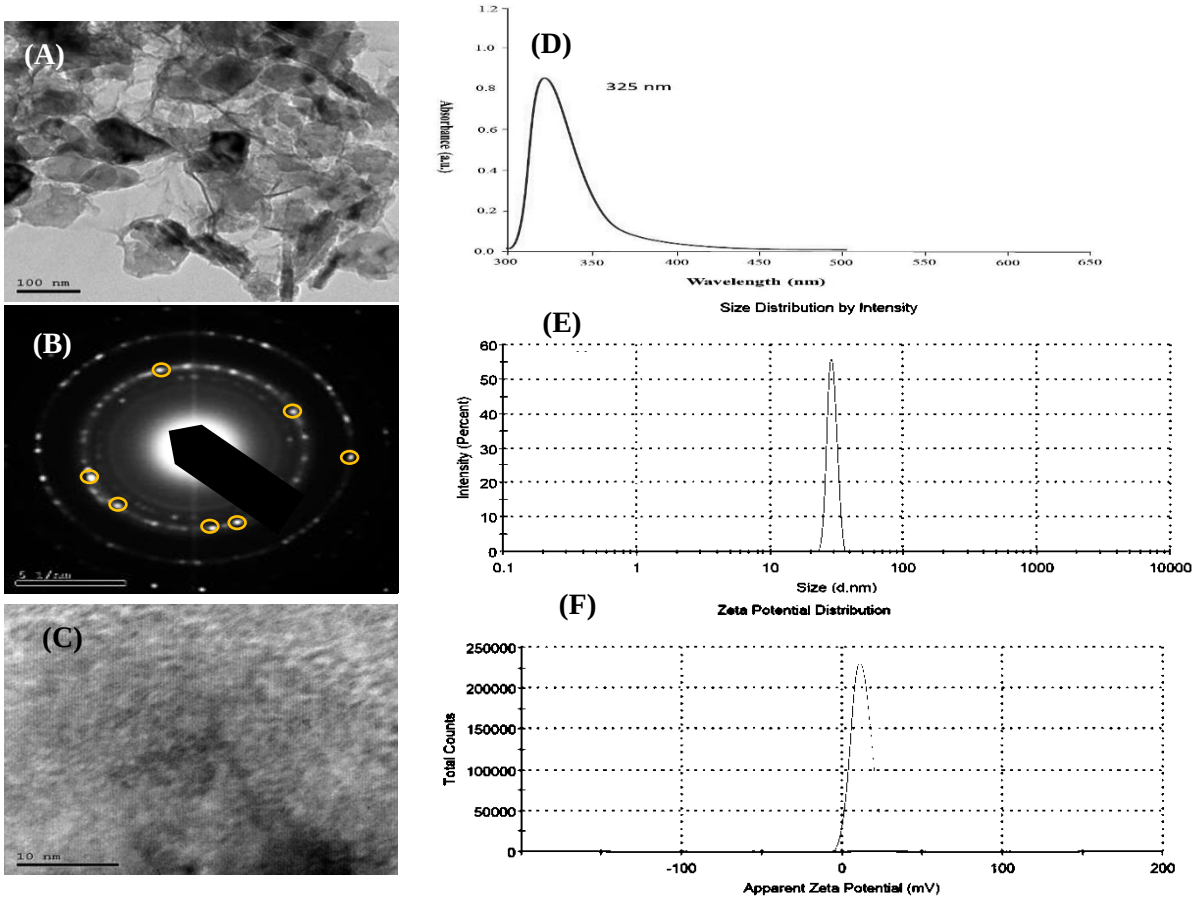

Figure 1. Characteristics of MgONPs synthesized by the reduction of MgONPs. (A) Representative image of transmission electron microscopy (TEM), (B) selected area electron diffraction (SAED) patterns in the inset (C), High-magnification view of MgONPs shows a lattice inter-planar spacing, (D) UV-vis spectra, (E) Size distribution, (F) Zeta potential measured by DLS.

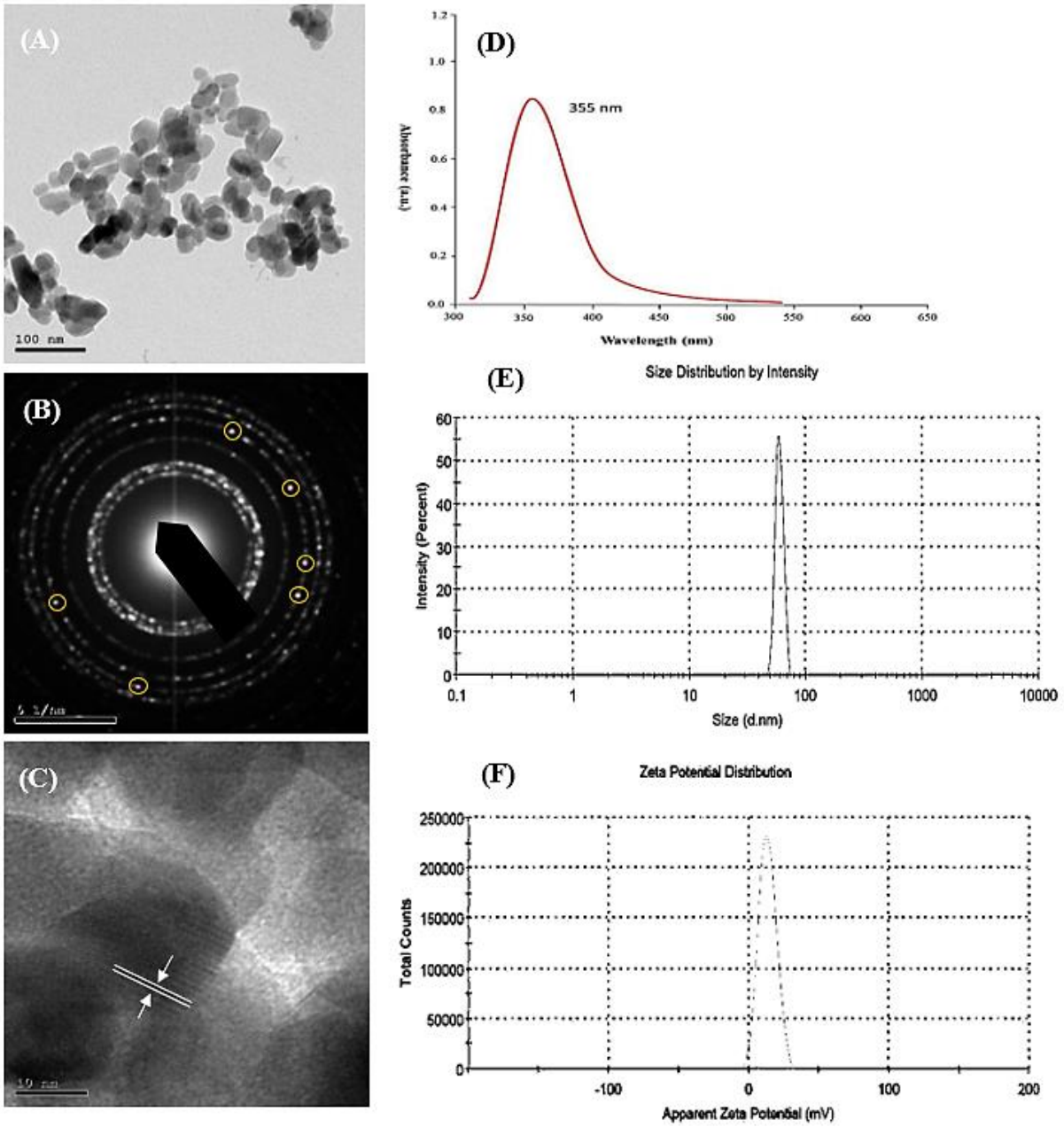

Figure 2. Characteristics of ZnONPs synthesized by the reduction of ZnONPs. (A) Representative image of transmission electron microscopy (TEM), (B) selected area electron diffraction (SAED) patterns (C), High-magnification view of ZnONPs shows a lattice inter-planar spacing, (D) UV-vis spectra, (E) Size distribution, (F) Zeta potential measured by DLS.

Antifungal Activity of MgONPs and ZnONPs Against Powdery Mildew on Pepper Under Greenhouse Conditions:

Data presented in Table (1) indicates that all treatments exhibited a reduction of final disease severity (FDS) compared to the control plants. The greatest reduction was obtained with treatment of MgONPs at 200 mg/L which significantly ($p<0.05$) reduced FDS (Table.1), and disease progress AUDPC (Table. 2) in the three greenhouses over other concentrations as well as control. Similarly, in the three greenhouses, treatment with ZnONPs was also effective in reducing FDS and disease progress AUDPC at concentration 200 mg/L in relative to other concentrations and control plants. The fungicide penconazole displayed the magnitude antifungal effect by recording the lowest values of FDS and AUDPC when compared with treatments of MgONPs, ZnONPs and control in all greenhouses (Table. 1 and 2). The LSD test at ($p<0.05$) revealed low significant difference in means of greenhouses, however, displayed a high significant difference between means of treatments as well as the interaction between treatments and the results of greenhouses.

Table 1. Final disease severity % (FDS) of powdery mildew in response to foliar treatments of MgONPs and ZnONPs in comparison with fungicide under greenhouse conditions

Treatment	Concentration (mg/ L)	FDS %			
		GH-1	GH-2	GH-3	Mean of treatments
MgONPs	100	16.13	18.55	15.61	16.76
	150	12.53	17.62	14.44	14.86
	200	11.72	12.25	11.73	11.90
ZnONPs	100	18.66	20.40	19.86	19.64
	150	16.47	18.48	16.36	17.10
	200	14.68	13.65	12.50	13.61
Penconazole	0.250 ml/L	10.26	10.51	10.06	10.28
Control		68.24	77.61	65.73	70.53
Mean of greenhouses		21.09	23.63	20.79	
$LSD_{at\ 0.05}$ Treatments = 1.120; Greenhouse = 0.686; Interaction = 1.941					

Table 2. Area under disease progress curve (AUDPC) of powdery mildew in response to foliar treatments of MgONPs and ZnONPs in comparison with fungicide under greenhouse conditions

Treatment	Concentration (mg/ L)	AUDPC %			
		GH-1	GH-2	GH-3	Mean of treatments
MgONPs	100	668.92	741.97	688.98	699.96
	150	642.71	689.64	633.22	655.19
	200	552.48	609.14	574.63	578.75
ZnONPs	100	728.42	813.51	791.07	777.67
	150	688.70	737.80	733.64	720.05
	200	614.08	673.75	663.74	650.52
Penconazole	0.250 ml/L	470.19	543.13	513.66	508.99
Control		1397.52	1727.57	1356.78	1493.96
Mean of greenhouses		720.38	817.06	744.47	
$LSD_{at\ 0.05}$ Treatments = 10.590; Greenhouse = 6.485; Interaction = 18.342					

Morphological Structures of Fungi Using SEM:

The disruption of cell integrity, especially the vegetative parts, could be observed on fungal structures of *O. sicula*. Also, deformation, shrinking and collapsing in fungal conidiophores and conidia with partially damaged cell walls were observed upon exposure to nanomaterials (Fig. 3A, B) over control (Fig. 3C, D). The conidia were predominantly dwindling in size and sometimes appeared swollen and lost its well-defined cylindrical to pyriform shape (white arrows) (Fig. 3A). The treatment with ZnONPs exhibited distinct inhibition of germinated conidia to make a new infection (white arrow) (Fig. 3B).

The Activity of Defence-Related Enzymes:

Data illustrated in Fig. (4) reveal that the activity of enzymes in pepper plants cv. Dolma was greatly increased in response to all treatments when compared to the control. Generally, pepper plants treated with MgONPs at the highest concentration of 200 mg/L exhibited the lowest peroxidase activities 0.541 ΔA422/10 sec/g FW in relation to control plants (Fig .4 A). Unlike, plants treated with ZnONPs at 200 mg/L displayed the highest peroxidase activities reached 1.016 ΔA422/10 sec/g FW over control (Fig .4 A, B). Out of all treatments, MgONPs at the highest concentration of 200 mg/L displayed the greatest activity of polyphenol oxidase with value reached 0.283 ΔA495/10 sec/g FW. While plants treated with penconazole showed the highest peroxidase activity among all treatments and recorded 1.229 ΔA422/10 sec/g FW (Fig. 3A).

Biochemical Assays:

All treatments resulted in a considerable increase in total chlorophyll when compared with the control plants (Fig. 5). There was no great variation among treatments in increasing total chlorophyll. Out of all treatments, MgONPs was superior in increasing total chlorophyll at the three concentrations with values 74.81, 82.94 and 91.19 mg/g FW, respectively (Fig .5).

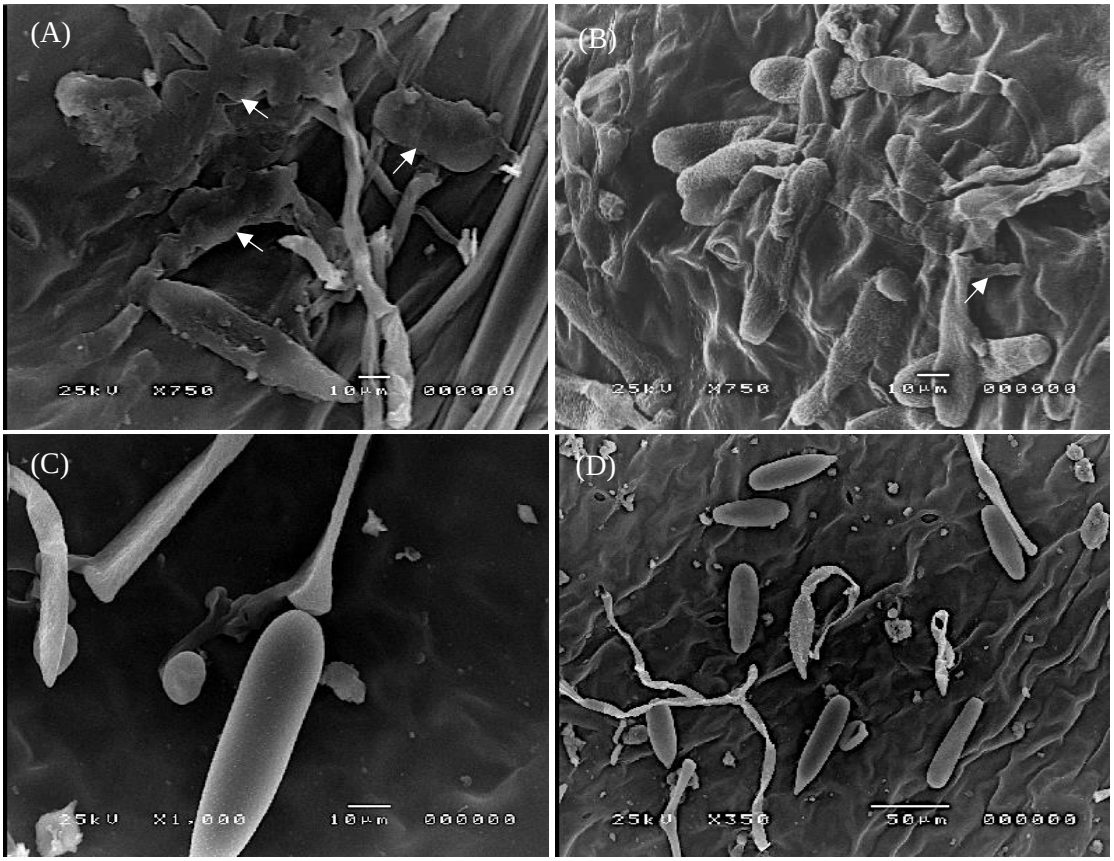

Figure 3. Scanning electron microscopy (SEM) observations of fungal structures of *O. sicula* sprayed with MgONPs (A), and ZnONPs (B) at 200 mg/L, 48 h after treatment and control (C and D).

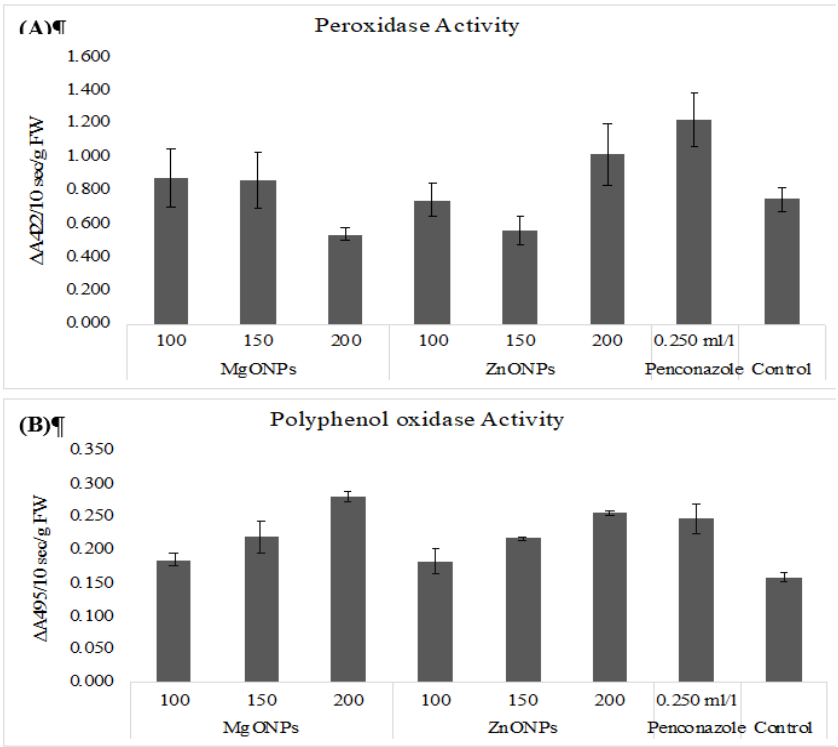

Figure 4. Enzyme activity of Peroxidase (A) and Polyphenol oxidase (B) in pepper plants 72 h. pretreatment with MgONPs, ZnONPs and penconazole under greenhouse conditions. Data represent the mean of 6 readings ± standar deviation at 10 sec intervals expressed as ΔA/10 sec/g FW.

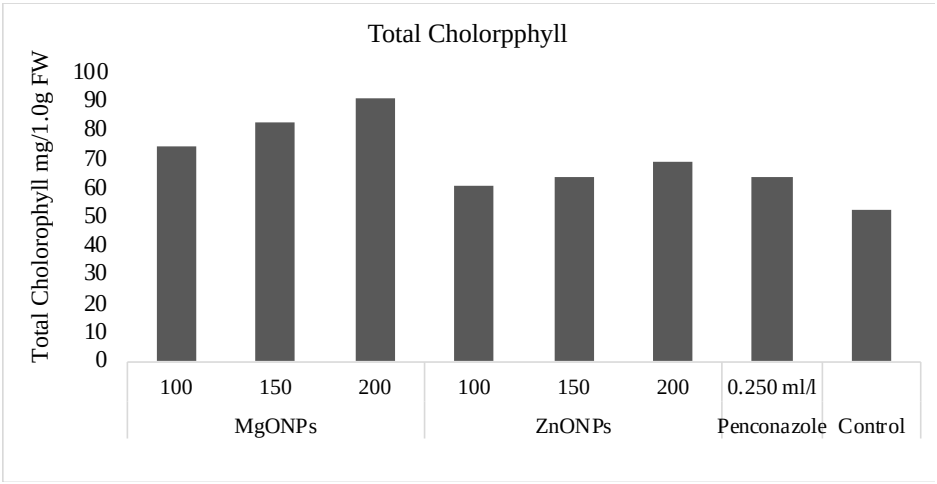

Figure 5. Total chlorophyll estimated in pepper leaves in response to foliar treatments with MgONPs, ZnONPs and penconazole under greenhouse conditions.

Cytotoxic Effect of MgONPs, ZnONPs and Penconazole Fungicide:

The cytotoxic effects were assessed based on MI and chromosomal aberration (CA) assay in meristematic cells of pepper. The MI values, frequency of mitotic phases, CA types and percentage, micronuclei types and numbers are given in Tables (4 and 5). The estimated score of MI of the pepper plants treated with MgONPs, ZnONPs and control are similar. According to the LSD test (Table 6), the combined data of the three greenhouses revealed a significant variation among treatments and control in terms of MI. Control plants exhibited the highest values of MI (17.54, 17.34 and 17.88) in GH-1, GH-2 and GH-3, respectively (Table 4). While, the lowest estimate in MI was obtained by the fungicide treatment in the three grenhouses (12.35, 13.36 and 12.67), respectively (Table 4). The frequency of each mitotic division phase was also studied, and no remarkable difference was observed in cell division phase at any concentration of MgONPs and ZnONPs (Table 4). However, penconazole fungicide illustrated a significant reduction in MI (Table 6) and frequency (%) of mitotic phases (Table 4).

Table 4. Mitotic index (MI) and frequency of mitotic phases in treated and control pepper plants

Locations	Treatments	Concentration (mg/ L)	No. of studied cells	No. of divided cells	MI	Frequency of mitotic phases %					
						Prophase		Metaphase		Ana-telophase	
						No.	%	No.	%	No.	%
GH-1	MgONPs	100	1400	229	16.36	80	5.71	71	5.07	78	5.57
		150	1410	235	16.67	79	5.60	69	4.89	87	6.17
		200	1350	226	16.74	78	5.78	70	5.19	78	5.78
	ZnONPs	100	1325	222	16.75	78	5.89	64	4.83	80	6.04
		150	1350	223	16.52	77	5.70	65	4.81	81	6.00
		200	1350	228	16.89	78	5.78	66	4.89	84	6.22
	Penconazole	0.250 ml/l	1320	163	12.35	61	4.62	48	3.64	54	4.09
	Control		1300	228	17.54	80	6.15	69	5.31	79	6.08
GH-2	MgONPs	100	1420	241	16.97	87	6.13	67	4.72	87	6.13
		150	1420	238	16.76	86	6.06	66	4.65	86	6.06
		200	1454	242	16.64	88	6.05	70	4.81	84	5.78
	ZnONPs	100	1450	240	16.55	84	5.79	68	4.69	88	6.07
		150	1470	248	16.87	89	6.05	70	4.76	89	6.05
		200	1450	245	16.90	88	6.07	72	4.97	85	5.86
	Penconazole	0.250 ml/l	1350	171	12.67	61	4.52	50	3.70	60	4.44
	Control		1398	250	17.88	81	5.79	80	5.72	89	6.37
GH-3	MgONPs	100	1440	240	16.67	79	5.49	77	5.35	84	5.83
		150	1450	235	16.21	81	5.59	74	5.10	80	5.52
		200	1405	236	16.80	80	5.69	76	5.41	80	5.69
	ZnONPs	100	1470	239	16.26	81	5.51	70	4.76	88	5.99
		150	1440	240	16.67	82	5.69	71	4.93	87	6.04
		200	1460	245	16.78	80	5.48	75	5.14	90	6.16
	Penconazole	0.250 ml/l	1400	187	13.36	60	4.29	58	4.14	69	4.93
	Control		1401	243	17.34	85	6.07	71	5.07	87	6.21

The estimated score of micronuclei and CA in response to foliar spray with MgONPs and ZnONPs, over control and fungicide are mainly similar (Table 5). All treatments induced CA at all tested concentrations. Abeerations, such as compact micronuclei (Fig. 6A), non-compact micronuclei (Fig. 6B), laggard chromosome (Fig. 6C), stickiness chromosome (Fig. 6D), binucleate cells (Fig. 6E), and fragment chromosome (Fig. 6F) were observed. There were differences among treatments in terms of CA %, ranged from the highest score of CA obtained by penconazole treatment which reached 12.80, to the lowest estimate in control plants with value 1.33. On the other hand, plants treated with ZnONPs reported low values 7.38 and 7.95 % of CA, followed by MgONPs, which recorded values ranged between 8.33 and 8.91 %. The statistical analysis of the combined data of the three greenhouses (Table 6), resulted in a significant variation among treatements in terms of number of CA and percentage. According to the LSD test, the penconazole treatment significantly increased number and percentage of CA over other treatments as well as control (Table .6).

Table 5. Frequency of micronuclei and CA in meristematic root-tips in treated and control pepper plants

Locations	Treatments	Concentration (mg/ L)	Total no. of studied cells	Types of micronuclei		No. of micronuclei	Types of chromosomal aberration				Chromosomal aberration	
				Compact	Non-Compact		Fragments	Stickiness	Binucleate cells	Laggard		
				No.	No.	No.	No.	No.	No.	No.	No.	%
GH-1	MgONPs	100	300	4	3	7	5	5	4	4	25	8.33
		150	321	4	4	8	5	6	5	4	28	8.72
		200	300	5	4	9	6	4	4	3	26	8.67
	ZnONPs	100	320	4	4	8	5	3	4	5	25	7.81
		150	335	5	3	8	5	4	4	5	26	7.76
		200	335	4	4	8	6	3	5	4	26	7.76
	Penconazole	0.250 ml/l	289	5	6	11	7	6	5	8	37	12.80
	Control		302	1	2	3	1	0	0	1	5	1.66
GH-2	MgONPs	100	321	4	5	9	4	5	4	5	27	8.41
		150	298	4	4	8	5	4	5	4	26	8.72
		200	258	3	4	7	5	4	4	3	23	8.91
	ZnONPs	100	288	3	4	7	4	3	4	4	22	7.64
		150	298	4	3	7	4	4	4	3	22	7.38
		200	302	4	4	8	5	3	4	4	24	7.95
	Penconazole	0.250 ml/l	294	5	5	10	7	6	6	8	37	12.59
	Control		300	1	1	2	0	0	1	1	4	1.33
GH-3	MgONPs	100	300	4	4	8	4	5	4	5	26	8.67
		150	290	3	4	7	5	4	4	5	25	8.62
		200	264	4	4	8	5	4	3	3	23	8.71
	ZnONPs	100	284	3	3	6	4	4	3	4	21	7.39
		150	265	4	3	7	3	3	4	4	21	7.92
		200	266	3	4	7	4	4	3	3	21	7.89
	Penconazole	0.250 ml/l	250	4	3	7	6	5	5	7	30	12.00
	Control		278	0	1	1	1	1	0	1	4	1.44

Table 6. Statistical analysis of MI and CA of the combined data of three greenhouses

Treatments	Concentration (mg/ L)	Mean of (GH-1, GH-2 and GH-3)		
		MI	No. of CA	CA %
MgONPs	100	16.67	26.00	8.47
	150	16.55	26.33	8.69
	200	16.73	24.00	8.76
ZnONPs	100	16.52	22.67	7.61
	150	16.69	23.00	7.69
	200	16.86	23.67	7.87
Penconazole	0.250 ml/L	12.79	34.67	12.46
Control		17.59	4.33	1.48
LSD at 0.05		0.50	2.87	0.41

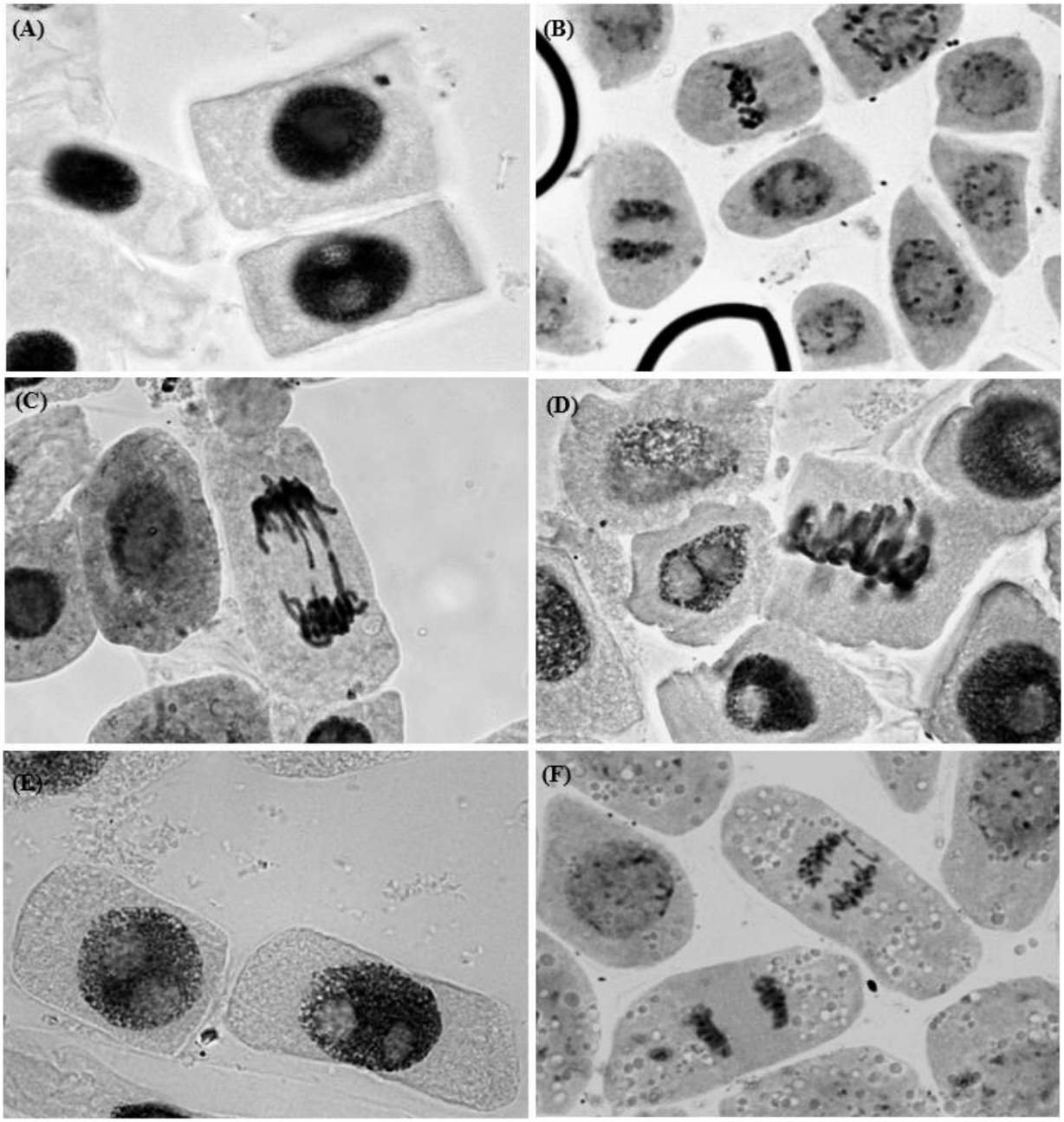

Figure 6. Microscopic analysis of CA in pepper root meristem cells; (A) Compact micronuclei, (B) Non-Compact micronuclei, (C) Laggard chromosome, (D) Stickiness chromosome, (E) Binucleate cells, (F) Fragment chromosome. All images were taken at 100X magnification.

DISCUSSION

The synthesis of ZnONPs was confirmed by UV absorption spectrum which exhibited a strong absorption band at 355 nm. This finding was supported by previous report of Talam *et al.* (2012) and was similar to the obtained results reported by Shamhari *et al.* (2018). Additionally, the UV spectrum exhibited an absorption peak at 325 nm to approve the formation of MgONPs. Previous studies reported that MgO exhibit a broad absorption peak between 260-330 nm (Rastogi *et al.,* 2015). The TEM results exhibited unsatisfactory dispensability of MgONPs due to agglomeration state, and the selected area electron diffraction (SAED) pattern confirmed crystalline nature and cubic shape of MgONPs. These findings were also reported in the study of Chen *et al.* (2020).

Considering the obtained results, the tested MgONPs and ZnONPs at the concentrations (100, 150 and 200 mg/L) significantly ($p<0.05$) reduced disease severity (DS) and calculated AUDPC in the three greenhouses over control. However, plants sprayed with MgONPs at higher dose exhibited results similar to penconazole fungicide. Hence, the antifungal effect of MgONPs could match the fungicide effect. More importantly, Imada *et al.* (2016), figured out that tomato plants treated before

infection with 350 µg/mL MgONPs showed a significant reduction in disease incidence caused by *Ralstonia solanacearum*. Whereas, the *in vitro* study of Cai *et al.* (2018b) MgONPs were shown to be considerably deadly to *R. solanacearum* at a concentration of 250 mg/L. Furthermore, Liao *et al*. (2019) found in a field experiment that treatment of MgONPs at 200 (g/mL greatly decreased disease severity of bacterial leaf spot on tomato. Furthermore, Parizi *et al*. (2014) demonstrated that MgONPs at 2% reduced the mycelial development of *Fusarium oxysporum* f. sp. *lycopersici*, the causative agent of tomato wilt, in the laboratory. In addition, Chen *et al.* (2020), demonstrated that application of MgONPs at 500 µg/mL significantly ($p<0.05$) reduced black shank and black root rot disease symptoms of tobacco caused by *Phytopthora nicotianae* and *Thielaviopsis basicola.* The study of Derbalah *et al.* (2013), indicated that foliar application of ZnONPs at 500 µg/mL reduced disease severity of Cercospora leaf blight of sugar beet.

The mode of MgONPs and ZnONPs action was not investigated in this study. However, earlier studies have attributed antifungal and bactericidal mechanisms to many theories (Xue *et al.,* 2014). Because of the arrangement of carboxyl and phosphate groups on the cell walls, the outer surface of the fungal mycelium is negatively charged at biological pH (Lee *et al*., 2004). MgONPs might be antifungal by directly acting on fungal cells, according to Chen *et al*. (2020). As a result, it's possible that positively charged MgONPs and ZnONPs have a close physical connection with fungus cells due to direct electrostatic adsorption. Cell membrane breakdown and cellular internalisation were encouraged as a result. Furthermore, we have shown that MgONPs produced lysis and cuts in the conidia and conidiophores cell wall due to sharp edges of NPs in high magnification SEM pictures, as corroborated by Xie *et al*. (2016) and Cai *et al*. (2018b). Instead, ZnONP penetration may cause greater internal ZnO-induced oxidative damage than outside the cells (Xue *et al*., 2014). This was in contrast to SEM micrograph, which suggested that ZnONPs' inhibitory action was due to cell death caused by NPs' penetration and deposition into cells without causing any physical damage. Additionally, ZnONPs suppressed germinated conidia to make new infection by forming aggregates on conidia surface through van der Waals forces as reported by Wang *et al.* (2014). Collectively, the effectiveness of ZnONPs as an antifungal is probably associated with translaminar movement.

Physiological and biochemical responses of pepper plants to treatments with MgONPs, ZnONPs and fungicides were estimated. According to Ruttkay-Nedecky *et al.* (2017), the chlorophyll contents are considered a critical parameter to analyze phytotoxicity. However, no toxicity was observed on pepper plants after two foliar sprays. Out of all treatments, only MgONPs resulted in a notable increase in total chlorophyll in pepper plants at 150 and 200 mg/L. Similarly, Cai *et al.* (2018a), found out that MgONPs increased the chlorophyll a and b contents in tobacco plants remarkably from 0.21 and 0.12 µg/g to 1.21 and 0.67 µg/g, respectively, after 30 days of treatment. Moreover, Raliya *et al.* (2014), demonstrated that biosynthesized MgONPs improved chlorophyll photosynthetic pigment with a value of 76.1% in cluster beans. By contrast, the results of Adjei *et al.* (2021), suggested that the low concentration of MgONPs increased the biosynthesis of chlorophyll in leaves whiles the high concentration decreased it. Unlike, treatments with ZnONPs had a lower effect on chlorophyll content in pepper plants than MgONPs, but still higher over fungicide and control. A relevant increase in chlorophyll content was obtained at a high concentration of 200 mg/L. On the contrary, Hussain *et al.,* (2021), found out that ZnONPs at higher concentrations (20 mg L^{-1}) decreased total chlorophyll content in leaves of *Persicaria hydropiper*. Also, Del Buono *et al.* (2021), proved that excessive dose of ZnONPs at 200 mg L^{-1} inhibited chlorophyll formation in Maize. The reduction in chlorophyll contents in metal-treated plants might be due to oxidation of photosynthetic pigments (Ma *et al.,* 2015).

The current results revealed that the higher concentrations (200 mg/L) of MgONPs negatively affected peroxidase activity. These results are supported with previously reported by Ramadan *et al.* (2020), who found that soybean plants sprayed with a higher concentration of 40 mg L^{-1} MgONPs, exhibited a low value of peroxidase activity. Conversely, Cai *et al.* (2018a), found that exposure of tobacco plants to 250 µg/mL of MgONPs enhanced the activity of peroxidase. While, the low concentrations of 50 and 150 µg/mL revealed lower activity. Whereas, our results exhibited the contrary, of which the low concentrations revealed higher activity and high concentrations revealed lower activity. Our results endorsed by previous findings of Farghaly *et al.* (2020), who stated that treatments of pomegranate callus tissues with ZnONPs at 150 µg mL^{-1} decreased the activity of peroxidase. On the other hand, the findings of Hussain *et al.* (2021) indicated that ZnONPs at a moderate concentration of 10 mg L^{-1} resulted in the optimum activity of peroxidase in *P. hydropiper* leaves. However, a concentration of 20 mg L^{-1} caused a decline in peroxidase activity. These results were similar with previous research that discovered negative effects of ZnONPs treatments on peroxidase activity in purslane roots (Iziy *et al.,* 2019). Low activities in antioxidant enzymes at the highest ZnONPs concentration could be attributed to the accumulation of free radicals in stressed plant tissues (Malar *et al.,* 2016). It was clear from our results that high levels of ZnONPs did not increase the activity of polyphenoloxidase. Conversely, the result of Farghaly *et al.* (2020), indicated that a high level of ZnONPs significantly stimulated the polyphenoloxidase activity in pomegranate callus tissues. Hence, ZnONPs displayed a dose-dependent response of antioxidant activity.

According to Hu *et al.* (2017), MI is a good indicator of cytotoxicity. The cytotoxicity of penconazole was evidenced in this work through a reduction in MI. Similarly, Bernardes *et al.* (2015) observed that difenoconazole-based formulation reduced the MI and increased the frequency of condensed nuclei. Furthermore, Kalefetoğlu Macar *et al.,* (2021), stated also, that the triazole fungicide diniconazole declined the MI and increased amount of CA. This was also consistent with previous research indicating that triazoles are mitotic division suppressors (Dubey *et al.,* 2015). The types observed in mitotic division were stickiness, fragments, laggards and binucleate cells. The same trend of our results was also reported by Seyhan *et al.* (2019), upon treatment of *Capsicum annuum* L. with Captan fungicide. Increased frequency of CA, (laggards and fragments), reduction of number of divided cells was highly induced by penconazole. Similar CA were reported by Aragão *et al.* (2019). Binucleus cell is another type of CA that was also observed as a result of penconazole treatment. Our result agreed with

those obtained by Demirtaş *et al.* (2015), who showed that binucleus cell is formed in meristematic roots of *Allium cepa* L. treated with diniconazole.

The recorded frequency of CA illustrated in Tables (4,5) and Fig (6), demonstrated that MgONPs and ZnONPs have cytotoxic effects on pepper. The treatments with MgONPs and ZnONPs at all concentrations had no great effect on MI when compared to control treatment. However, Kumari *et al.* (2011), reported that ZnONPs reduced the MI in meristematic tissue of *Allium cepa*. Likewise, El-Ghamery *et al.* (2016), found out that ZnO at bulk and nanoparticles form caused reduction in MI of *Allium cepa* and induced different types of CA. All tested concentrations induced CA with slight differences. An earlier study of chromosomal morphology discovered a link between increasing the number of abnormalities and increasing the concentration of NPs (Arruda *et al.,* 2015). Bilal *et al.* (2017), supported this investigation and observed a substantial decrease in the MI from 60.30% to 27.62% with increasing concentration of the NPs. Mangalampalli *et al*. (2017) discovered the sole study in the literature that highlighted the cytotoxic impact of MgONPs on *Allium cepa* root cells. The decrease and rise in CA were shown to be directly related to the concentration and indirectly proportional to the size of MgO particles. On the contrary, alterations observed in this study were not proportional to the concentration of the tested nanomaterials.

CONCLUSION

In the current work, MgONPs and ZnONPs were shown to be viable alternatives to fungicides for controlling powdery mildew in peppers grown in greenhouses. MgONPs, at greater doses, produced outcomes that were similar to penconazole fungicide. Fortunately, none of the nanomaterials tested on pepper plants showed phytotoxicity throughout the testing. MgONPs and ZnONPs had no negative impacts on pepper plants, such as leaf deformation, curling, chlorosis, or necrosis. The antifungal toxicity characteristics can be related mostly to nanoparticle–cell direct contact, which has traditionally been detected utilising SEM technologies, as well as oxidative stress. Future research is needed to determine the effects of MgONPs and ZnONPs at various concentrations on edible plants, as well as their bioaccumulation in edible parts.

Acknowledgments:

The authors would like to thank and appreciate the efforts done in proofreading this work by Prof. Dr. Aly Abdel Hady, Prof. Dr. Abdel Mohsen Tohamy, and Prof. Dr. Kamel Abd-Elalam.

REFERENCES

Abdel-Kader, M.M., El-Mougy, N.S., Aly, M.D.E., Lashin, S.M., & Abdel-Kareem, F. (2012). Greenhouse biological approach for controlling foliar diseases of some vegetables. *Advances in Life Sciences*, 2(4), 98–103.

Adjei, M.O., Zhou, X., Mao, M., Xue, Y., Liu, J., Hu, H., Luo, J., Zhang, H., Yang, W., Feng, L., & Ma, J. (2021). Magnesium Oxide nanoparticle effect on the growth, development, and microRNAs expression of *Ananas comosus var. bracteatus*. *Journal of Plant Interactions*, 16:1, 247-257.

Bilal, A., Dwivedi, S., Zainul Abdin, M., Azam, A., Al-Shaeri, M., Khan, M.S., Saquib, Q., Al-Khedhairy, A.A., & Musarrat, J. (2017). Mitochondrial and chromosomal damage induced by oxidative stress in Zn2+ Ions, ZnO-Bulk and ZnO-NPs treated *Allium cepa* roots. *Scientific Reports*, 7, 1-14.

Alghuthaymi, M.A., Kalia, A., Bhardwaj, K., Bhardwaj, P., Abd-Elsalam, K.A., Valis, M., & Kuca, K. (2021). Nanohybrid antifungals for control of plant diseases: Current status and future perspectives. *Journal of Fungi*, 7, 1-20.

Allam, A. I., & Hollis, J. P. (1972) Sulfide inhibition of oxidases In rice roots. *Phytopathology*, 62, 634-636.

Aragão, F.B., Bernardes, P.M., Ferreira, A., Da Silva Ferreira, M.F., & Andrade-Vieira, L.F. (2019). Cyto(geno)toxicity of commercial fungicides based on the active compounds tebuconazole, difenoconazole, procymidone, and iprodione in *Lactuca sativa* L. meristematic Cells. *Water, Air, Soil and Pollution,* 230, 1-9.

Arnon, D. I. (1949). Copper enzymes in isolated chloroplasts. Polyhenoloxidases in *Beta vulgaris*. *Plant Physiology*, 24, 1-15.

Arruda, S.C., Silva, A.L., Galazzi, R.M., Azevedo, R.A., & Arruda, M.A. (2015). Nanoparticles applied to plant science: A review. *Talanta*, 131, 693–705.

Bernardes, P.M., Andrade-Vieira, L.F., Aragão, F.B., Ferreira, A., & Da Silva Ferreira, M. F. (2015). Toxicity of difenoconazole and tebuconazole in *Allium cepa*. *Water, Air, and Soil Pollution*, 226, 1-11.

Cai, L., Liu, M., Liu, Z., Yang, H., Sun, X., Chen, J., Xiang, S., & Ding, W. (2018a). MgONPs Can Boost Plant Growth: Evidence from Increased Seedling Growth, Morpho-Physiological Activities, and Mg Uptake in Tobacco (*Nicotiana tabacum* L.). *Molecules*, 23, 1-15.

Cai, L., Chen, J,. Liu, Z., Wang, H., Yang, H., & Ding, W. (2018b). Magnesium Oxide Nanoparticles: Effective Agricultural Antibacterial Agent Against *Ralstonia solanacearum*. *Frontiers in Microbiolology*, 9, 1-19.

Chen, J., Wu, L., Lu, M., Lu, S., Li, Z., & Ding, W. (2020). Comparative study on the fungicidal activity of metallic MgO nanoparticles and macroscale MgO against soilborne fungal phytopathogens. *Frontiers in Microbiolology*, 11, 1-19.

Del Buono, D., Di Michele, A., Costantino, F., Trevisan, M., & Lucini, L. (2021). Biogenic ZnO Nanoparticles synthesized using a novel plant extract: Application to enhance physiological and biochemical traits in Maize. *Nanomaterials*, 11, 1-15.

Demirtaş, G., Çavusoglu, K., & Yalçin, E. (2015). Anatomic, physiologic and cytogenetic changes in *Allium cepa* L. induced by diniconazole. *Cytologia*, 80, 51–57.

Derbalah, A.S., El-Moghazy, S.M., & Godah, M.I. (2013). Alternative control methods of sugar beet leaf spot disease caused by the fungus *Cercospora betticola* (Sacc). *Egyptian Journal of Biology and Pest Control*, 23, 247-254.

Descalzo, R.C., Rohe, J.E., & Mauza, B. (1990). Comparative efficacy of induced resistance to selected diseases of greenhouse cucumber. *Canadian Journal of Plant Pathology*, 12, 69-79.

Dubey, P., Mishra, A.K., Shukla, P., & Singh, A.K. (2015). Differential sensitivity of barley (*Hordeum vulgare* L.) to chlorpyrifos and propiconazole: morphology, cytogenetic assay and photosynthetic pigments. *Pesticide Biochemistry and Physiology*, 124, 29–36.

El-Ghamery, A.A., Abdel-Azeem, E.A., El-Kholy, M.A., & Gamal El-Dein, O.A. (2016). A comparative study for the cytological effect of ZnO nanoparticles and ZnO bulk on *Allium cepa* L. *Nature and Science*, 14, 87-96.

Elmer, W., & White, J.C. (2018). The future of nanotechnology in plant pathology. *Annual Review of Phytopathology*, 56, 111-133.

Farghaly, F.A., Radi, A.A., Al-Kahtany, F.A., & Hamada, A.F. (2020). Impacts of zinc oxide nano and bulk particles on redox-enzymes of the *Punica granatum* callus. *Scientific Reports*, 10, 1-13.

FDA. (2016). Part 182- Substances generally recognized as safe. (accessed 2021 Septemper 11). Available from: Available from: https://www.ecfr.gov/current/title-21/chapter-I/subchapter-B/part-182.

Guigón López, C., García Ramírez, H.A., & Muñoz Castellanos, L.N. (2020). Control of Pepper Powdery Mildew Using Antagonistic Microorganisms: An Integral Proposal. In: Mérillon, J.M., Ramawat, K.G. (eds) Plant Defence: Biological Control. *Progress in Biological Control*, 22, 385-420.

Guigón-López, C., Muñoz-Castellanos, L., Ortiz, N., & González, J. (2018). Control of powdery mildew (*Leveillula taurica*) using *Trichoderma asperellum* and *Metarhizium anisopliae* in different pepper types. *BioControl*, 64.

Gunalana, S., Sivaraja, R., & Rajendran, V. (2012). Green synthesized ZnO nanoparticles against bacterial and fungal pathogens. Progress in Natural Science: *Materials International*, 22, 693 – 700.

Hu, Y., Tan, L., Zhang, S-H., Zuo, Y-T., Han, X., Liu, N., Lu, W.Q., & Liu, A.L. (2017). Detection of genotoxic effects of drinking water disinfection by-products using *Vicia faba* bioassay. *Environmental Science and Pollution Research*, 24,1509–1517.

Hussain, F., Hadi, F., & Rongliang, Q. (2021). Effects of zinc oxide nanoparticles on antioxidants, chlorophyll contents, and proline in *Persicaria hydropiper* L. and its potential for Pb phytoremediation. *Environmental Science and Pollution Research*, 28, 34697–34713.

Imada, K., Sakai, S., Kajihara, H., Tanaka, S., & Ito, S. (2016). Magnesium oxide nanoparticles induce systemic resistance in tomato against bacterial wilt disease. *Plant Pathology*, 65, 551-560.

Iziy, E., Majd, A., Vaezi-Kakhki, M.R., Nejadsattari, T., & Noureini, S.K. (2019). Effects of zinc oxide nanoparticles on enzymatic and nonenzymatic antioxidant content, germination, and biochemical and ultrastructural cell characteristics of *Portulaca oleracea* L. *Acta Societatis Botanicorum Poloniae*, 88, 1-14.

Jacobs, T.W. (1997). Why do plant cells divide?. *Plant Cell*, 9,1021-1029.

Jin, T., & He, Y.P. (2011). Antibacterial activities of magnesium oxide (MgO) nanoparticles against foodborne pathogens. *Journal of Nanoparticle Research*, 13, 6877–6885.

Kalefetoğlu Macar, T., Macar, O., Yalçın, E., & Çavuşoğlu, K. (2021). Preventive efficiency of Cornelian cherry (*Cornus mas* L.) fruit extract in diniconazole fungicide-treated *Allium cepa* L. roots. *Scientific Reports*, 11, 1-9. https://doi.org/10.1038/s41598-021-82132-4.

Kalia, A., Abd-Elsalam, K.A., & Kuca, K. (2020). Zinc-Based Nanomaterials for Diagnosis and Management of Plant Diseases: Ecological Safety and Future Prospects. *Journal of Fungi*, 6, 1-29.

Köhler, J.M., Abahmane, L., Wagner, J., Albert, J., & Mayer, G. (2008). Preparation of metal nanoparticles with varied composition for catalytical applications in microreactors. *Chemical Engineering Science*, 63, 5048–5055.

Krishnamoorthy, K., Moon, J.Y., Hyun, H.B., Cho, S.K., & Kim, S.J. (2012). Mechanistic investigation on the toxicity of MgO nanoparticles toward cancer cells. *Journal of Material Chemistry*, 22, 24610–24617.

Kumari, M., Khan, S.S., Pakrashi, S., Mukherjee, A., & Chandrasekaran, N. (2011). Cytogenetic and genotoxic effects of zinc oxide nanoparticles on root cells of *Allium cepa*. *Journal of Hazardous Materials*, 190, 613–621.

Lee, S.A., Willeke, K., Mainelis, G., Adhikari, A., Wang, H., Reponen, T., & Grinshpun, S.A. (2004). Assessment of electrical charge on airborne microorganisms by a new bioaerosol sampling method. *Journal of Occupational and Environmental Hygiene*, 1, 127–138.

Liao, Y.Y., Strayer-Scherer, A.L., White, J., Mukherjee, A., De La Torre-Roche, R., Ritchie, L., Colee, J., Vallad, G.E., Freeman, J.H., Jones, J.B., & Paret, M.L. (2019). Nano-Magnesium Oxide: A Novel Bactericide Against Copper-Tolerant *Xanthomonas perforans* Causing Tomato Bacterial Spot. *Phytopathology*, 109, 52-62.

Ma, C., White, J.C., Xing, B., & Dhankher, O.P. (2015). Phytotoxicity and ecological safety of engineered nanomaterials. *International Journal of Plant and Environment*, 1, 9–15.

Malandrakis, A.A., Kavroulakis, N., & Chrysikopoulos, C.V. (2019). Use of copper, silver and zinc nanoparticles against foliar and soil-borne plant pathogens. *Science of The Total Environment*, 670, 292–299.

Malar, S., Vikram, S.S., Favas, P.J., & Perumal, V. (2016). Lead heavy metal toxicity induced changes on growth and antioxidative enzymes level in water hyacinths [*Eichhornia crassipes* (Mart.)]. *Botanical Studies*, 55, 54–65.

Mangalampalli, B., Dumala, N., & Grover, P. (2017). Allium cepa root tip assay in assessment of toxicity of magnesium oxide nanoparticles and microparticles. *Journal of Environmental Sciences*, 66:125-137.

Matta, A.I., & Dimond, A.F. (1963). Symptoms of Fusarium wilt in relation to quantity of fungus and enzyme activity in tomato stems. *Phytopathology*, 53, 574-578.

Pandey, H.N., Menon, T.C.M., & Rao, M.V. (1989). A simple formula for calculating area under disease progress curve. London: Barely and Wheat Newsletter.

Parizi, M.A., Moradpour, Y., Roostaei, A., Khani, M., Negahdari, M., & Rahimi, G. (2014). Evaluation of the antifungal effect of magnesium oxide nanoparticles on *Fusarium oxysporum* F. sp. *lycopersici*, pathogenic agent of tomato. *European Journal of Experimental Biology*, 4, 151–156.

Pernezny, K., Roberts, P.D., Murphy, J.F., & Goldberg, N.P. (2003). Compendium of Pepper Diseases. The American Phytopathological Society, APS Press, 63 pp.

Porra, R.J. (2005). The chequered history of the development and use of simultaneous equations for the accurate determination of chlorophylls a and B. In: Discoveries in photosynthesis. Springer; p. 633–640. http://link.springer.com/chapter/10.1007/1-4020-3324-9_56

Raliya, R., Tarafdar, J.C., Singh, S.K., Gautam, R., Choudhary, K., Maurino, V. G., & Saharan, V. (2014). MgO nanoparticles biosynthesis and its effect on chlorophyll contents in the leaves of clusterbean (*Cyamopsis tetragonoloba* L.). *Advanced Science Engineering and Medicine*, 6, 538–545.

Ramadan, A.B., El-Bassiouny, H.M.S., Bakry, B.A., Abdallah M.M.S., & El-Enany, M.A.M. (2020). Growth, Yield and Biochemical Changes of Soybean Plant in Response to Iron and Magnesium Oxide Nanoparticles. *Pakistan Journal of Biological Sciences,* 23: 406-417.

Rastogi, C.K., Saha, S., Sivakumar, S., Pala, R.G.S., & Kumar, J. (2015). Kinetically stabilized aliovalent europium-doped magnesium oxide as a UV sensitized phosphor. *Physical Chemistry Chemical Physics*, 17, 4600–4608.

Sayed-Ahmed, M.S. (1985). Genetical and cytogenetical studies in broad bean (*Vicia faba* L.). M.Sc. Thesis, Fac. Agric. Zagazig University, Egypt.

Seyhan, M., Yüzbaşıoğlu, E., Dalyan, E., Akpınar I., & Ünal, M. (2019). Genotoxicity and Antioxidant Enzyme Activities Induced by the Captan Fungicide in the Root of Bell Pepper (*Capsicum annuum* L. var. *grossum* L. cv. Kandil). *Trakya University Journal of Natural Sciences*, 20, 97-103.

Shamhari, N.M., Wee, B.S., Chin, S.F., & Kok, K.Y. (2018). Synthesis and Characterization of Zinc Oxide Nanoparticles with Small Particle Size Distribution. *Acta Chimica Slovenica*, 65, 578-585.

Spencer, D.M. (1977). Standard Methods for Evaluation of fungicides for the control of cucurbits powdery mildew. In Mac Farlane, M.R. Crop Protection agents and their biological evaluation. Academic Press London. 455 - 464.

Talam, S., Karumuri S.R., & Gunnam, N. (2012). Synthesis, Characterization, and Spectroscopic Properties of ZnO Nanoparticles. *International Scholarly Research Notices*, 2012, 1-6.

Tamilselvi, P., Yelilarasi, A., Hema, M., & Anbarasan, R. (2013). Synthesis of hierarchical structured MgO by sol-gel method. *Nano Bulletin*, *2*(1), 1-5.

Wagner, G., Korenkov, V., Judy, J.D., & Bertsch, P.M. (2016). Nanoparticles composed of Zn and ZnO inhibit *Peronospora tabacina* spore germination in vitro and *P. tabacina* infectivity on tobacco leaves. *Nanomaterials*, 6, 1-10.

Wang, X. P., Liu, X.Q., Chen, J.N., Han, H.Y., & Yuan, Z.D. (2014). Evaluation and mechanism of antifungal effects of carbon nanomaterials in controlling plant fungal pathogen. *Carbon*, 68, 798–806.

Wightwick, A., Walters, R., Allinson, G., Reichman, S., & Menzies, N. (2010). Environmental risks of fungicides used in horticultural production systems. Fungicides, Odile Carisse (Ed.), ISBN: 978-953-307-266-1.

Xie, J.R., Ming, Z., Li, H.L., Yang, H., Yu, B., Wu, R. Liu, X., Bai, Y., & Yang, S.T. (2016). Toxicity of graphene oxide to white rot fungus *Phanerochaete chrysosporium*. *Chemosphere*, 151, 324–331.

Xue, J., Luo, Z., Li, P., Ding, Y., Cui, Y., & Wu, Q. (2014). A residue-free green synergistic antifungal nanotechnology for pesticide thiram by ZnO nanoparticles. *Scientific Reports*, 4, 1-9.

النشاط المضاد للفطريات للجسيمات النانومترية لاكسيدالمغنيسيوم و الزنك على البياض الدقيقي فى الفلفل تحت ظروف الصوبة

احمد محمود إسماعيل[١*]، منى إبراهيم عبد الجواد[٢]
[١]معهد بحوث أمراض النباتات، مركز البحوث الزراعية، مصر
[٢] معمل الوراثة الخلوية، البنك القومي للجينات، مركز البحوث الزراعية، مصر
*بريد المؤلف المراسل: ma.ah.ismail@gmail.com

الملخص

يعتبر مرض البياض الدقيقي للفلفل المتسبب عن فطر *Oidiopsis sicula* من الامراض الضارة في الحقل والصوب. وتعتبر المكافحة الكيميائية هي الأكثر استخداما على نطاق واسع لمكافحة البياض الدقيقي. ولتقليل الآثار الضارة للمبيدات الفطرية، هدفت الدراسة الحالية إلى تقييم التأثير المضاد للتركيزات المختلفة (100، 150 و200 مجم / لتر) من MgONPs وZnONPs ضد البياض الدقيقي مقارنة بالمبيد الفطري penconazole (0.25 مل / لتر) تحت ظروف الصوبة. تم تخليق وتعريف الجزيئات النانومترية ل MgONPs وZnONPs والكشف عنها باستخدام تحليل DLS والذي اثبت وجود هذه المواد في الصورة النانومترية بمتوسط حجم 52.97 نانوميتر ± 1.43 SD و79.45 نانوميتر ± 1.74 SD، على التوالي. تم تطبيق المواد النانومترية وذلك بالرش مرتين بمعدل رشة واحدة كل أسبوعين على نباتات الفلفل صنف (دولما)، مصابة بمرض البياض الدقيقي في الصوب الانتاجية الثلاثة بالدقي (GH-1)، طوخ (GH-2) والهرم (GH-3). أظهرت المعاملات بكل من MgONPs وZnONPs انخفاضا ملحوظا للشدة المرضية (DS) والمنطقة الواقعة تحت منحنى تقدم المرض (AUDPC) عند استخدامهم بتركيز 200 مجم / لتر. أظهر التحليل الإحصائي فرقاً معنوياً ($P < 0.05$) بين المعاملات في الصوب الثلاثة وكذلك بين متوسطات المعاملات المدمجة للصوب الثلاثة. كما أظهرت صور الميكروسكوب الالكتروني الماسح التأثير المثبط والمميت ل MgONPs وZnONPs لجراثيم وميسليوم فطر *Oidiopsis sicula*. أظهرت نباتات الفلفل التي تم معاملتها بالمبيد الفطري penconazole أعلى نشاط لأنزيم peroxidase وسجلت 1.229 ΔA422/10 sec/g FW. بينما، نباتات الفلفل التي تم معاملتها ب MgONPs أظهرت أعلى نشاط لأنزيم polypheneloxidase بقيمة وصلت 0.283 ΔA495/10 sec/g FW. وكانت المعاملة ب MgONPs، هي الأفضل في زيادة الكلوروفيل الكلي عند التركيزات الثلاثة التي تم تقييمها، بقيم 74.81 و82.94 و91.19 مجم / جم FW على التوالي. واظهرت اختبارات السمية الجينية ان MgONPs، ZnONPs والمبيد الفطري penconazole لها تأثير سام ومثبط للانقسام الخلوي لخلايا جذور الفلفل. النتائج المتحصل عليها من هذه الدراسة اثبتت إمكانية استخدام MgONPs وZnONPs كبديل للمبيدات الكيماوية التقليدية.

الكلمات المفتاحية: سمية الخلايا ، الجسيمات النانومترية لاكسيدالمغنيسيوم و الزنك ، الفلفل ، البياض الدقيقي